Evidence of two-stage melting of Wigner solids

Talbot Knighton, Zhe Wu, and Jian Huang*
Department of Physics and Astronomy, Wayne State University, Detroit, Michigan 48201, USA

Alessandro Serafin and J. S. Xia
Department of Physics and National High Magnetic Field Laboratory, University of Florida, Gainesville, Florida 32611-8440, USA

L. N. Pfeiffer and K. W. West
Department of Electrical Engineering, Princeton University, Princeton, New Jersey 08544, USA

(Received 10 September 2017; revised manuscript received 11 November 2017; published 20 February 2018; corrected 26 September 2018)

Ultralow carrier concentrations of two-dimensional holes down to $p = 1 \times 10^9$ cm^{-2} are realized. Remarkable insulating states are found below a critical density of $p_c = 4 \times 10^9$ cm^{-2} or $r_s \approx 40$. Sensitive dc *V-I* measurement as a function of temperature and electric field reveals a two-stage phase transition supporting the melting of a Wigner solid as a two-stage first-order transition.

DOI: 10.1103/PhysRevB.97.085135

A Wigner crystal (WC) [1] of electrons in two dimensions is a long-sought-after phenomenon driven by strong electron-electron interaction and the melting of a WC provides a unique opportunity of understanding the solid-liquid transition (SLT) [2–4]. According to the Monte Carlo calculations, a WC occurs when the ratio of the interparticle Coulomb energy E_{ee} and the Fermi energy E_F, $r_s = E_{ee}/E_F = a/a_B$, is at least 37 [5]. $a = 1/\sqrt{\pi n}$ is the Wigner-Seitz radius for electron density n and $a_B = \hbar^2\epsilon/m^*e^2$ is the Bohr radius. Therefore, in order to observe a WC, the charge concentrations must be extremely dilute, i.e., $\leqslant 1 \times 10^9$ cm^{-2} for electrons or $\leqslant 4 \times 10^9$ cm^{-2} for holes in GaAs two-dimensional (2D) systems. Experiments in such small electron energy limits are challenging because the disorder effects, unless effectively suppressed, easily overwhelm the interaction-driven effects. Natural consequences are the Anderson localization [6], glass states [7], and mixed phases; all of which do not possess true long-range correlations. As a result, neither a WC nor a melting transition has been clearly demonstrated. Most detection efforts target collective modes and have so far produced only softly pinned modes undergoing a second-order-like thermal melting. These modes, as broadly suspected, could easily result from intermediate or mixed phases (e.g., hexatics, bubbles/stripes, or glass phases) since the observed correlation lengths (ξ), corresponding to the sizes of WCs, are usually small. Clear evidence of a WC demands not only demonstrations of longer or even macroscopic ξ, but, moreover, a melting transition marked by a singularity [8–10]. This work presents evidence for collective pinning modes characterized by a macroscopic ξ, as well as two-stage SLT, analogous to the Kosterlitz-Thouless (KT) model [4,10–15], except for a first-order transition suggested by a discontinuity across the critical point.

Most WC studies adopt the reentrant and quantum Hall insulating phases (RIP and QHIP) in a large magnetic field (B) where interaction effect is enhanced without reaching an ultradilute limit. Detection of the collective modes has been conducted with respect to pinning [16–18] and resonant absorption (via rf, microwaves, acoustic waves [19–22], tunneling [23]). However, there lacks evidence distinguishing a WC from intermediate/mixed phases. In fact, the estimated ξ is not only small (up to 1 μm), but also decays exponentially with increasing temperature (T) in a fashion similar to what is expected for an intermediate phase (i.e., hexatics [13,24]). Similar results are also obtained through studies in zero-B fields [25–27]. Zero-B results at $r_s > 40$ are quite rare due to the requirement for far more dilute carrier densities where disorder effect is even more prominent because the screening effect is weak as the interparticle spacing, $a = 1/\sqrt{\pi n} \sim$ 200–500 nm, approaches the screening length. This is why even fairly clean systems become highly insulating when n is $\sim$8–9 $\times 10^9$ cm^{-2} [27,28]. Consequently, r_s is limited to 5–15. Therefore, disorder suppression, as supported by almost all experiments, remains the key to successful detection of WCs.

In addition to driving a localization, another subtle disorder effect is its influence on the WC melting temperature (T_m), i.e. via fluctuations that break long-range translational symmetry. This less understood effect could alter current models of melting such as the KT model and is expected to be more effective in suppressing T_m than the quantum fluctuations [9,10]. Disorder suppression is therefore key in keeping T_m accessible. Most reported $T_m \sim$ 100–200 mK for small ξ cases are likely the crossover points between the intermediate/mixed and the liquid phases. To probe a transition, i.e., from a WC-intermediate phase, requires cooling to lower T.

This study focuses on the dc transport response of collective pinning and melting in ultrahigh-quality dilute 2D systems. A proven cooling method using a helium-3 immersion cell is adopted [29]. Key observations include enormously pinned collective modes, characterized by a differential resistance (r_d) of $\sim$1.3 GΩ, that exhibit a remarkable threshold nonlinear dc *I-V* identical to pinned charge density waves (CDWs). The

*Corresponding author: jianhuang@wayne.edu

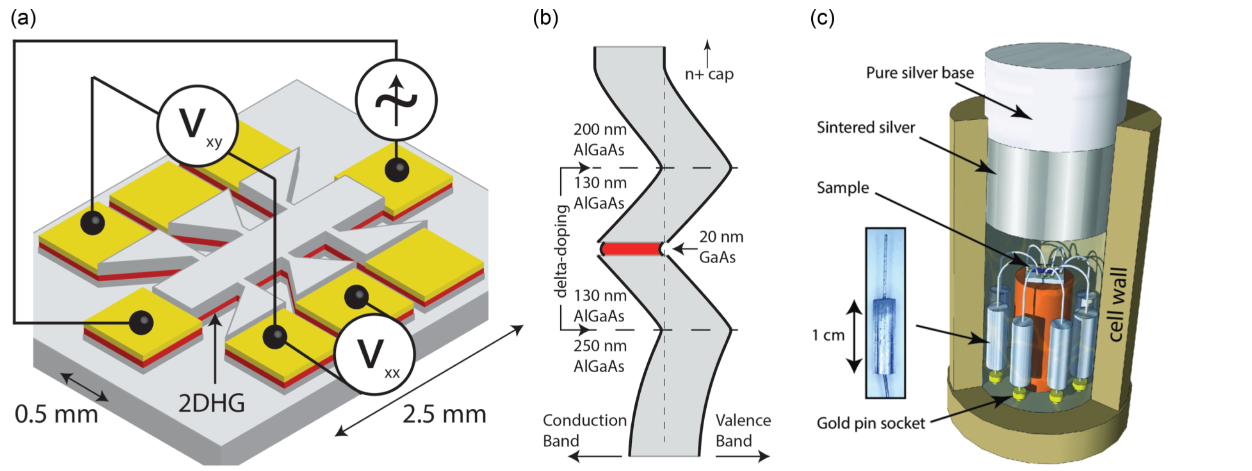

FIG. 1. (a) Sample dimensions and measurement configuration. (b) Band diagram of the quantum square well. (c) Cooling schematics inside a helium-3 immersion cell.

critical temperature is $T_m \sim 35$ mK. Moreover, heating across T_m results in a discontinuity in r_d which supports a first-order two-stage thermal melting. The presentation is divided into two parts: The first is a study of the RIP near filling $\nu = 1/3$ using p-doped quantum wells, and the second is a zero-B-field study of ultradilute holes in undoped heterojunction-insulated-gate field-effect transistors (HIGFETs) at $r_s \geqslant 40$.

The samples used for the RIP measurement are lightly doped p-type (100) GaAs quantum wells patterned into a 2.5×0.5 mm Hall bar. The density p is $\sim 4 \times 10^{10}$ cm^{-2} ($r_s = 24$), with mobility of $\mu \approx 2.5 \times 10^6$ cm^2/V s. Thermally deposited AuBe pads annealed at 460 °C achieve excellent Ohmic contacts to the 2D carriers, with measured contact resistances ∼400 Ω. Measurements are performed in a dilution refrigerator inside a shielded room, allowing minimal electronic noises.

Cooling dilute carriers to 10 mK is challenging because sample thermalization relies mainly on cooling through the sample leads (via *ee* interaction) because the phonon modes are frozen out. We have established an effective cooling method via a helium-3 sample immersion cell and achieved 5 mK cooling GaAs 2D holes as dilute as $p = 5 \times 10^9$ cm^{-2} [29]. The carrier density for the RIP study here is nearly ten times higher. The cell is mounted at the lower end of a cold finger with its top fastened to the mixing chamber (mc) plate [Fig. 1(c)]. The roof is a sintered silver cylindrical-block extension made by compressed pure silver microparticles. During operation, helium-3 gas is continuously fed through a capillary into the cell where it condenses to fill the volume completely. Saturated sintered silver block provides ∼30 m^2 contact area to cool the helium-3 bath. Major cooling of the 2D holes is realized via efficiently heat-sinking the metal contacts through sintered silver pillars providing 2.5 m^2 surface area per lead. T is monitored through a helium-3 melting curve thermometer. The T differential between the bath and the mc is $\leqslant 0.1$ mK at all times.

Figure 2(a) shows the magnetoresistance (MR) (ρ_{xx}) and the Hall resistance (ρ_{xy}) measured at 10 mK via a four-terminal ac technique. The inset shows the Shubnikov de Haas (SdH) oscillations starting at 0.05 T. The RIP peak centers at $B =$ 4.5 T ($\nu = 0.375$) between fillings $\nu = 2/5$ and $1/3$, with a dip in ρ_{xy} consistent with previous studies [30,31]. $B = 4.5$ T corresponds to a magnetic length $l_B = \sqrt{hc/eB} \approx 28$ nm equal to $a = 1/\sqrt{\pi p}$. This is where a WC is expected. However, we found that dc techniques, instead of the ac techniques, are the appropriate method probing the RIP peak because, as shown later, it is essential to measured bulk resistance r with currents of ∼1 pA which are far below the offset limits in the ac driving signals. An electrometer-level dc setup is therefore adopted with a voltage bias V between ±10 mV (at 0.1 μV resolutions). Current sensing via a low-noise preamp provides 50 fA precision.

Cooling to 9 mK, dc *IV* within a ±5 nA window displays a sharp threshold [inset of Fig. 2(b)] apparently identical to a pinned CDW [32]. The differential resistance $r_d = dV/dI$ within the threshold $V_c \sim 1$ meV is approximately 1.3 GΩ, with nearly no current flow ($I \leqslant$ 1–2 pA). This supports a collective pinning below a threshold electric field $E_c = V_c/L \sim 10$ mV/cm because the single-particle energy $w_c = eE_c a \sim 0.024$ μeV (or 0.3 mK) is significantly smaller than T. $L \sim 0.5$ mm is the distance between the voltage leads and $a = 1/\sqrt{\pi p} = 28$ nm is the average charge spacing. However, current is switched on immensely at a critical current I_c and r_d plummets by nearly 6000 times. It indicates a phase transition occurring at a remarkably small threshold current $I_c \sim 2$ pA. This electric field (E)-driven phase transition becomes more evident in the later T-dependent results. Joule heating is $< 10^{-15}$ W and thus negligible.

Another important evidence that supports a crystal phase is a melting transition which several studies have reported around 150–300 mK [16–23,25–27]. Figure 2(b) shows *IV*s with each of the curves corresponding to a fixed T between 10 and 300 mK. The threshold behavior is robust up to ∼40 mK, with $r_d \sim$ 1–1.3 GΩ and $I_c \sim$ 2–3 pA. For higher T, the threshold behavior is replaced with rounded nonlinear *IV*s between 40 and 140 mK with substantially suppressed $r_d \sim$ MΩ. Eventually, linear *IV* is restored beyond 140 mK which is commonly recognized as a liquid phase due to the absence of pinning.

Naturally, a phase transition can be driven by both T and I (or V). Therefore, caution must be taken when examining the thermal melting because the sheet resistance $r = V/I$ are

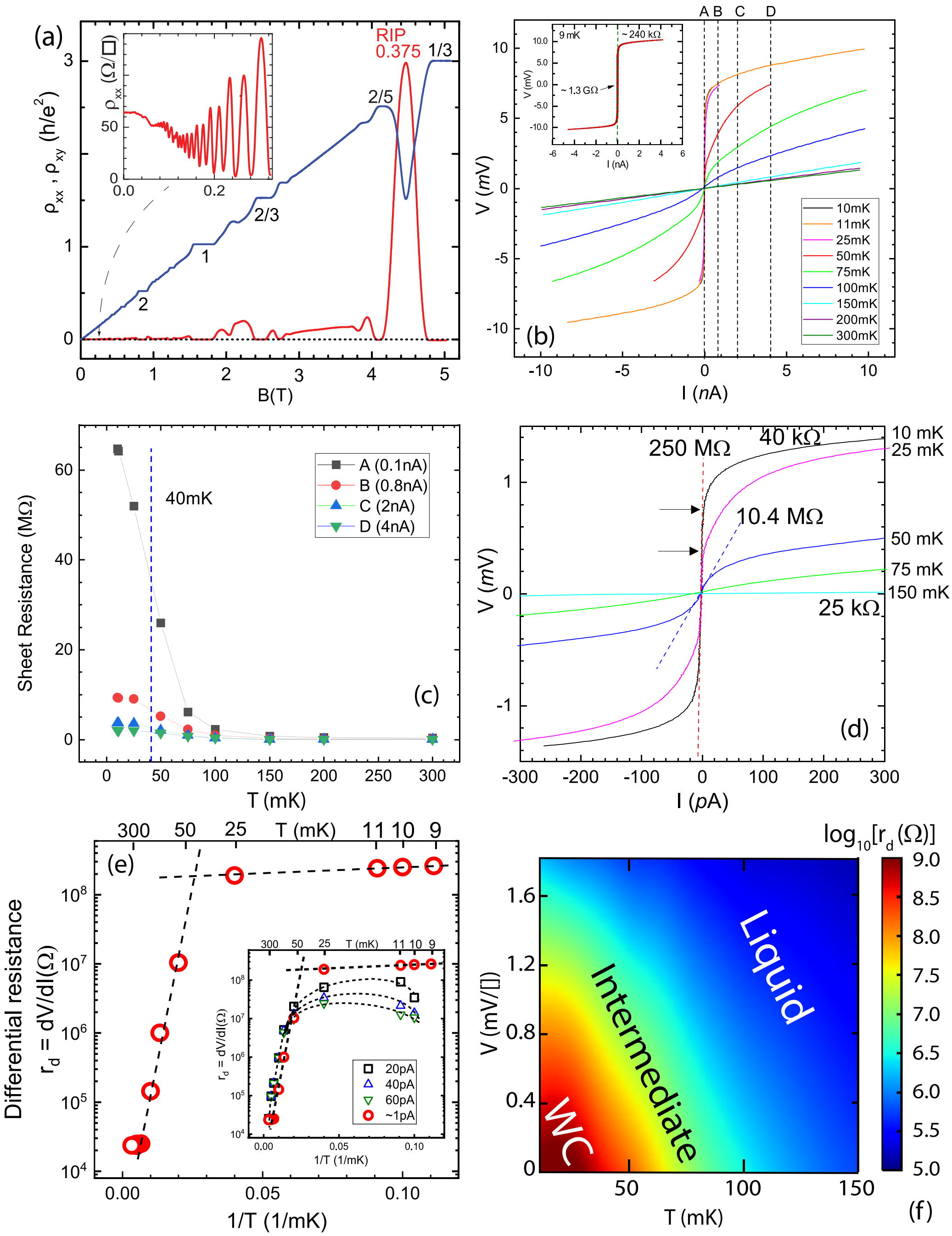

FIG. 2. (a) MR and Hall resistance at 10 mK. Inset: SdH oscillations. (b) dc *IV* measured at $B = 4.5$ T at various T from 10 to 300 mK. Inset: *IV* at 9 mK. (c) T dependence of the resistance (V/I) measured with 0.1, 0.8, 2, and 4 nA driving currents. (d) Amplified view of (b) for a narrower current range. (e) Piecewise T dependence of $r_d(T) = dV/dI|_{V\to 0}$ on semilogarithmic scales. Inset: comparison to $r_d(T)$ obtained with higher current drives. Dotted lines are guides. (f) Suggested contour phase diagram based on $\log_{10} r_d(T)$ values.

extremely sensitive to the level of the drives down to picoampere limits. For a demonstration, $r(T)$s obtained at four different randomly picked current drives, labeled by the dotted lines in Fig. 2(b), are plotted in Fig. 2(c). For $I \geqslant 1$ nA, $r(T)$ varies little with increasing I, consistent with a liquid phase behavior. However, $r(T)$ exhibits more than two orders increase already with $I \sim 100$ pA which must be linked to a transition effect.

Therefore, thermal melting must be examined in the limit of $I \to 0$. Figure 2(e) shows $r_d(T)|_{I\to 0}$ in comparison to the $r_d(T)$ obtained at 20, 40, and 60 pA. $r_d(T)|_{I\to 0}$ is well described as a piecewise behavior across a critical temperature of $\sim$35 mK defined as T_m. r_d decreases with increasing T at a rate of 1.5 MΩ/mK for $T \leqslant T_m$. For $T \geqslant T_m$, r_d exhibits an exponential dive marked by nearly four orders of magnitude down to 150 mK. The abrupt change within a few millikelvins of T_m is referred to as a discontinuity that supports, also confirmed by the zero-field results shown later, a possible first-order phase transition. The piecewise $r_d(T)$, however, disappears with I increased just beyond I_c. As shown in the inset of Fig. 2(e), $r_d(T)$ measured between

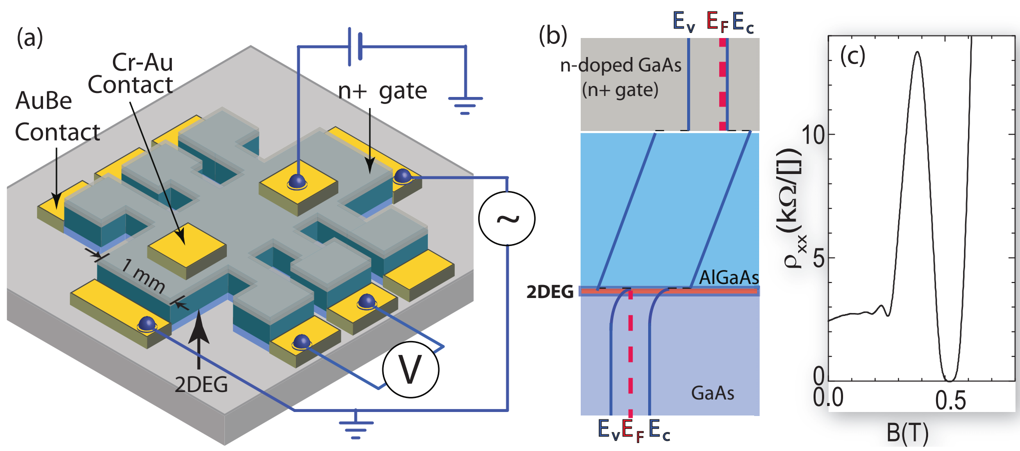

FIG. 3. (a) HIGFET sample and measurement schematics. (b) Band diagram showing accumulation of holes at the GaAs/AlGaAs junction. (c) $\rho_{xx}(B)$ for $p = 1.2 \times 10^{10}$ cm^{-2}.

20 and 60 pA is substantially suppressed at $T \leqslant T_m$ and only smooth nonmonotonic crossovers are found. These results are consistent with what is indicated by the threshold behavior that a phase transition has occurred when $I > I_c$.

Meanwhile, although pinning at $T < T_m$ is consistently strong, V_c exhibits a noticeable T dependence. Figure 2(d) shows selected *IV*s for 10, 25, 50, 75, and 150 mK within a narrower window. Note that r_d is now shown as resistivity (instead of resistance). For 10 and 25 mK, current switches on at different thresholds: 0.4 mV for 25 mK and 0.8 mV for 10 mK. Lower E_c for higher T is qualitatively consistent with the Lindemann criterion for crystal melting [14]. An estimate of ξ is provided here, similar to previous studies [18,33], based on a pinning model [34,35] that balances the pinning energy with the electrical potential energy $U = Nw_c$. $w_c = eE_c a \sim 0.024$ μeV $\ll T$ is the single-particle potential energy. $N = p\xi^2$ is the number of carriers on a scale of ξ. For $T = 25$ mK, $E_c = V_c/L \sim 8$ mV/cm where $L = 0.5$ mm. Setting the electrical force NeE_c equal to the pinning force κa [17,18], κ being the shear modulus $0.245e^2p^{3/2}/4\pi\epsilon_0\epsilon$ [36], $N \sim 1.5 \times 10^5$ or $\xi \geqslant 10$ μm is obtained. U is $\sim$2.4 meV (or 30 K), comparable to E_{ee}.

For T between 40 and 140 mK, the threshold is replaced with a rounded nonlinear *IV*. This observation is in agreement with several previous results [17,25–27] which were interpreted as pinned WCs. However, E_c disappears because a current switches on in the limit of $V \to 0$. In addition, pinning is substantially reduced, i.e., $r_d \sim 10$ MΩ at 50 mK. Therefore, this region should be of an intermediate phase since it crosses over to a liquid above 140 mK (referred to as T_l). r_d for $T \geqslant T_l$ is 30–40 k$\Omega/\square$. The same values of r_d are found for the liquid phase arrived at by E-field-driven melting at sufficiently large bias. A suggested phase diagram is shown in Fig. 2(f).

To identify the nature of the intermediate phase is difficult because the exact relationship between r_d and $\xi(T)$ has to first be formulated. Here, as a minor point, we show that $r_d(T)$ can be fitted to $r_d = r_0 \exp[c/(T - 40\text{ mK})^\gamma]$ with $r_0 \approx 23$ and $c \approx 9.5$, in the same trend as the exponentially decreasing

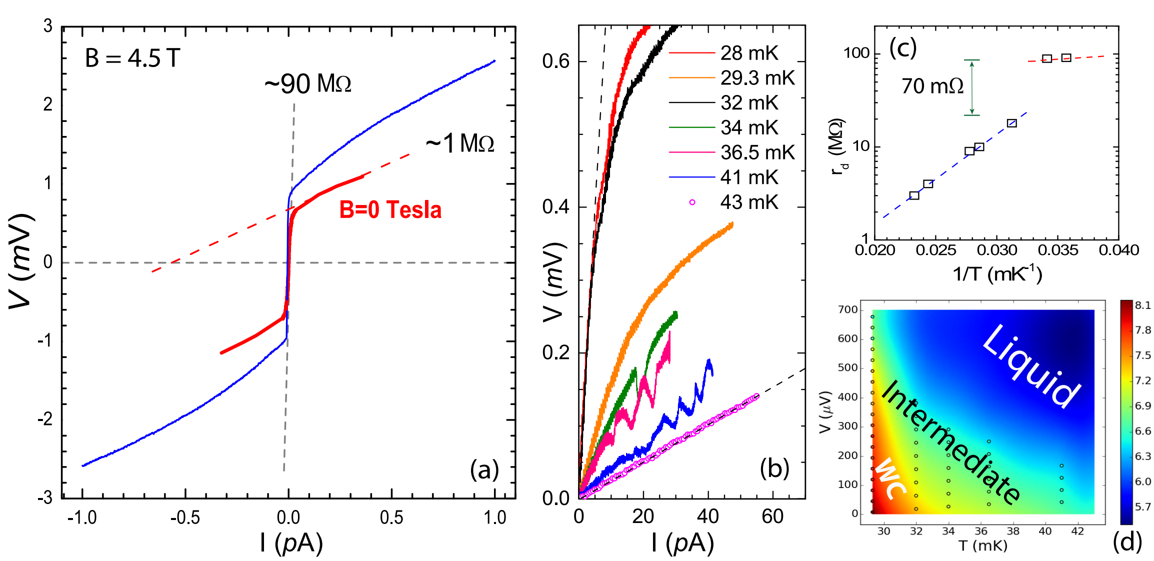

FIG. 4. (a) dc *IV* at $T = 28$ mK. (b) *IV*s obtained at different T. (c) T dependence of $r_d(T)|_{V\to 0}$ on semilogarithmic scales. (d) Colored contour phase diagram based on $\log_{10} r_d(T)$ values. Dashed lines are guides.

$\xi(T)$ modeled for a hexatic phase [13]: $\xi \sim \exp[c/(T - T_m)^{\gamma}]$ ($\gamma \approx 0.3696$).

We now turn to the zero-B-field study with undoped GaAs/AlGaAs HIGFETs [37–39]. A 6 mm $\times$ 0.8 mm Hall bar is realized with a self-align fabrication process [39] [Fig. 3(a)]. Accumulation of holes at the heterointerface is capacitively induced through biasing a top gate beyond a turn-on voltage, ~ -1.3 V, at which the valance band edge meets the chemical potential [Fig. 3(b)]. The band gap of the 600-nm-thick $Al_{0.3}Ga_{0.7}As$ barrier is ~2 eV. Owing to the superior crystal quality, gate leakage remains less than 0.05 pA at all operating bias. Density p, determined via quantum Hall oscillations [Fig. 3(c)], is tunable from 4×10^{10} down to 7×10^{8} cm^{-2}.

Accessing $r_s \geqslant 40$ requires $p \leqslant 4 \times 10^9$ cm^{-2}. $m^* = 0.25m_0$ is a lower-bound estimate. (Determination of m^* is difficult because of a complicated dispersion relation associated with the light-heavy hole band mixing and the spin-orbit coupling [40].) It is thus important to exclude disorder-driven localization which easily occurs as phonon-activated hopping $\rho(T) \sim \rho_0 \exp{(T^*/T)^{1/\beta}}$ ($\beta = 1$–3) [41,42]. Recent studies of ultraclean systems revealed nonactivated power-law behaviors [38,43,44] of interaction-driven nature that distinguishes from a disorder-driven effect. And, the metal-to-insulator transition (MIT) [45] occurs at lowest carrier densities corresponding to $r_s \sim 35$–40. We refer the readers to Refs. [38,43,44,46] for details.

The measured MIT in zero B (not shown) has a critical density $p_c = 4 \times 10^9$ cm^{-2}. The following dc results are for $p = 2.8 \times 10^9$ cm^{-2} (or $r_s \sim 45$) measured between 28 and 45 mK. A current bias, with Keithley 6430 fA source, is employed with a voltage sensing at sub-μV resolution at an input impedance of 10^{16} Ω. Figure 4(a) shows a similar threshold *IV* obtained at 28 mK, qualitatively identical to the RIP case. I_c is ~4 pA. Strong subthreshold pinning is marked by a r_d of 90 M$\Omega/\square$. The suprathreshold r_d collapses 100 times. I_c corresponds to a $E_c \sim 4$ mV/cm (or $\sim 10^{-10}$ V/a_B), yielding a slightly larger single-particle potential energy of $\sim eE_c a \sim 0.04$ μeV (or 0.46 mK) due to the larger $a \sim 100$ nm. Setting $NeE_c = \kappa a$ as shown earlier, one obtains $N \sim 1 \times 10^5$, corresponding to a substantial scale of $\xi \sim 100$ μm. This yields a dominating potential energy $U \sim 20$ meV $> E_{ee}$ which is consistent with a crystal. For a consistency check, the same setup is used to measure the RIP and the result is shown as the blue curve. The power dissipation is $\leqslant 2 \times 10^{-16}$ W, ruling out appreciable Joule heating.

Melting probed by $r_d|_{I\to 0}$ is shown in Fig. 4(c) where a piecewise behavior appears across $T_m \sim 30$ mK. dr_d/dT is 4 MΩ/mK for $T < T_m$. r_d exhibits a sharp jump of 70 MΩ at T_m above which an exponential T dependence is found. E_c disappears at $T > T_m$ where rounded nonlinear *IV* is found. The discontinuous jump resembles a recent quantum Monte Carlo simulation for a first-order WC-intermediate phase transition mediated by a discontinuous internal energy jump [10], and supports a singularity dividing a WC from an intermediate phase. Linear *IV* is recovered at $T_l \sim 42$ mK, noticeably lower than the RIP case. Smaller T_m and T_l for the ultradilute case is qualitatively consistent with stronger quantum fluctuations and disorder fluctuations (due to lack of screening). A phase diagram is suggested in Fig. 4(d).

Increasing E-field results in a switch-on of current and a settlement of r_d belonging to a liquid phase. Identical to the RIP case, a melting mediated by an intermediate phase is supported. However, there is a noticeable difference in the intermediate phase at $T > T_m$: V oscillates with increasing I at approximately 5–10 pA spacing. It occurs more frequently as T approaches T_l [Fig. 4(b)]. The formation of stripes with long-range orientational order [13], as seen in electrons on a helium surface [47], could be a possible cause. Another possibility is that small T_l facilitates a melting and recrystallization of pinned WC domains, instead of or in addition to shearing, when driven across pinning sites [48]. This will contribute to a negative r_d.

To summarize, enormous pinning modes below T_m support a WC on large ξ scales. A melting is captured as a two-stage SLT. The WC-intermediate phase transition is likely first-ordered [10] because of the discontinuity in r_d as well as the disappearance of E_c above T_m. Results obtained from both RIP and zero-B-field studies are remarkably consistent. The small T_m, which is $\sim(1/7)T_{cm}$, suggests strong effects from system disorders and quantum fluctuations that require further understanding.

This work is supported by NSF under Grant No. DMR-1410302, by the Gordon and Betty Moore Foundation through Grant No. GBMF2719, and by NSF Grant No. MRSEC-DMR-0819860. A portion of this work was performed at the National High Magnetic Field Laboratory, which is supported by National Science Foundation Cooperative Agreement No. DMR-1644779 and the State of Florida.

[1] E. Wigner, Phys. Rev. **46**, 1002 (1934).
[2] N. D. Mermin and H. Wagner, Phys. Rev. Lett. **17**, 1133 (1966).
[3] N. D. Mermin, Phys. Rev. **176**, 250 (1968).
[4] J. Kosterlitz and D. Thouless, J. Phys. C **5**, L124 (1972).
[5] B. Tanatar and D. M. Ceperley, Phys. Rev. B **39**, 5005 (1989).
[6] P. W. Anderson, Phys. Rev. **109**, 1492 (1958).
[7] H. Aoki, J. Phys. C **12**, 633 (1979).
[8] P. Anderson, *Basic Notions of Condensed Matter Physics* (Benjamin/Cummings, Menlo Park, CA, 1984).
[9] M. Takahashi and M. Imada, J. Phys. Soc. Jpn. **53**, 3765 (1984).
[10] B. K. Clark, M. Casula, and D. M. Ceperley, Phys. Rev. Lett. **103**, 055701 (2009).
[11] J. M. Kosterlitz and D. J. Thouless, J. Phys. C **6**, 1181 (1973).
[12] B. I. Halperin and D. R. Nelson, Phys. Rev. Lett. **41**, 121 (1978).
[13] D. R. Nelson and B. I. Halperin, Phys. Rev. B **19**, 2457 (1979).
[14] G. M. Bruun and D. R. Nelson, Phys. Rev. B **89**, 094112 (2014).
[15] A. P. Young, Phys. Rev. B **19**, 1855 (1979).
[16] H. W. Jiang, H. L. Stormer, D. C. Tsui, L. N. Pfeiffer, and K. W. West, Phys. Rev. B **44**, 8107 (1991).

[17] V. J. Goldman, M. Santos, M. Shayegan, and J. E. Cunningham, Phys. Rev. Lett. **65**, 2189 (1990).
[18] F. I. B. Williams, P. A. Wright, R. G. Clark, E. Y. Andrei, G. Deville, D. C. Glattli, O. Probst, B. Etienne, C. Dorin, C. T. Foxon, and J. J. Harris, Phys. Rev. Lett. **66**, 3285 (1991).
[19] E. Y. Andrei, G. Deville, D. C. Glattli, F. I. B. Williams, E. Paris, and B. Etienne, Phys. Rev. Lett. **60**, 2765 (1988).
[20] Y. P. Chen, G. Sambandamurthy, Z. H. Wang, R. M. Lewis, L. W. Engel, D. C. Tsui, P. D. Ye, L. N. Pfeiffer, and K. W. West, Nat. Phys. **2**, 452 (2006).
[21] H. Zhu, Y. P. Chen, P. Jiang, L. W. Engel, D. C. Tsui, L. N. Pfeiffer, and K. W. West, Phys. Rev. Lett. **105**, 126803 (2010).
[22] M. A. Paalanen, R. L. Willett, P. B. Littlewood, R. R. Ruel, K. W. West, L. N. Pfeiffer, and D. J. Bishop, Phys. Rev. B **45**, 11342 (1992).
[23] J. Jang, B. M. Hunt, L. N. Pfeiffer, K. W. West, and R. C. Ashoori, Nat. Phys. **13** 340 (2017).
[24] D. R. Nelson and B. I. Halperin, Phys. Rev. B **21**, 5312 (1980).
[25] S. V. Kravchenko, J. A. A. J. Perenboom, and V. M. Pudalov, Phys. Rev. B **44**, 13513 (1991).
[26] V. M. Pudalov, M. D'Iorio, S. V. Kravchenko, and J. W. Campbell, Phys. Rev. Lett. **70**, 1866 (1993).
[27] J. Yoon, C. C. Li, D. Shahar, D. C. Tsui, and M. Shayegan, Phys. Rev. Lett. **82**, 1744 (1999).
[28] M. Y. Simmons, A. R. Hamilton, M. Pepper, E. H. Linfield, P. D. Rose, D. A. Ritchie, A. K. Savchenko, and T. G. Griffiths, Phys. Rev. Lett. **80**, 1292 (1998).
[29] J. Huang, J. S. Xia, D. C. Tsui, L. N. Pfeiffer, and K. W. West, Phys. Rev. Lett. **98**, 226801 (2007).
[30] T. Sajoto, Y. P. Li, L. W. Engel, D. C. Tsui, and M. Shayegan, Phys. Rev. Lett. **70**, 2321 (1993).
[31] M. Hilke, D. Shahar, S. Song, D. Tsui, Y. Xie, and D. Monroe, Nature (London) **395**, 675 (1998).
[32] G. Grüner, Rev. Mod. Phys. **60**, 1129 (1988).
[33] V. J. Goldman, M. Shayegan, and D. C. Tsui, Phys. Rev. Lett. **61**, 881 (1988).
[34] P. A. Lee and H. Fukuyama, Phys. Rev. B **17**, 542 (1978).
[35] H. Fukuyama and P. A. Lee, Phys. Rev. B **17**, 535 (1978).
[36] L. Bonsall and A. Maradudin, Phys. Rev. B **15**, 1959 (1977).
[37] B. E. Kane, L. N. Pfeiffer, and K. W. West, Appl. Phys. Lett. **67**, 1262 (1995).
[38] H. Noh, M. P. Lilly, D. C. Tsui, J. A. Simmons, E. H. Hwang, S. Das Sarma, L. N. Pfeiffer, and K. W. West, Phys. Rev. B **68**, 165308 (2003).
[39] J. Huang, D. S. Novikov, D. C. Tsui, L. N. Pfeifer, and K. W. West, Int. J. Mod. Phys. B **21**, 1219 (2007).
[40] R. Winkler, *Spin–Orbit Coupling Effects in Two-Dimensional Electron and Hole Systems* (Springer, New York, 2003).
[41] N. F. Mott, Philos. Mag. **19**, 835 (1969).
[42] A. L. Efros and B. I. Shklovskii, J. Phys. C **8**, L49 (1975).
[43] J. Huang, D. S. Novikov, D. C. Tsui, L. N. Pfeiffer, and K. W. West, Phys. Rev. B **74**, 201302 (2006).
[44] J. Huang, L. N. Pfeiffer, and K. W. West, Phys. Rev. B **85**, 041304 (2012).
[45] S. V. Kravchenko, W. E. Mason, G. E. Bowker, J. E. Furneaux, V. M. Pudalov, and M. D'Iorio, Phys. Rev. B **51**, 7038 (1995).
[46] J. Huang, L. N. Pfeiffer, and K. W. West, Phys. Rev. Lett. **112**, 036803 (2014).
[47] P. Glasson, V. Dotsenko, P. Fozooni, M. J. Lea, W. Bailey, G. Papageorgiou, S. E. Andresen, and A. Kristensen, Phys. Rev. Lett. **87**, 176802 (2001).
[48] B. G. A. Normand, P. B. Littlewood, and A. J. Millis, Phys. Rev. B **46**, 3920 (1992).